2*k*-Grating-assisted self-pumped phase conjugation: theoretical and experimental studies

Shiuan Huei Lin,* Ying Wu Lian,† and Pochi Yeh

Electrical and Computer Engineering Department, University of California, Santa Barbara, California 91306

Ken Y. Hsu

Institute of Electro-Optical Engineering, National Chiao Tung University, Hsinchu, Taiwan

Zhu Yong

Institute of Physics, Chinese Academy of Sciences, Beijing, China

Received November 1, 1995

We investigated 2*k*-grating-assisted self-pumped phase conjugation in photorefractive Ce:$BaTiO_3$ crystals. The phase-conjugation process involves a combination of four-wave mixing and stimulated photorefractive backscattering. An approximation involving separate interaction regions is used to theoretically calculate the reflectivity of phase conjugation as a function of the coupling strength of four-wave mixing and stimulated photorefractive backscattering. In our experiments, grating-erasure techniques are employed at the interaction regions to investigate the dependence of phase-conjugate reflectivity on the coupling strength of four-wave mixing and stimulated photorefractive backscattering. The experimental results are in good agreement with the theoretical prediction.

Key words: Self-pumped phase conjugate, stimulated photorefractive backscattering, four wave mixing.

1. INTRODUCTION

In self-pumped phase conjugators the counterpropagating beams needed in a four-wave-mixing process are generated by the incident beam itself. By a process that is not entirely understood, the self-generated pump beams are often formed in a configuration tending to optimize the phase-conjugated beam. Self-pumped phase conjugators have been demonstrated in a variety of configurations. Two classes of self-pumped phase conjugator have been proposed and demonstrated: the passive self-pumped phase conjugator, which needs externally aligned mirrors,[1] and the true self-pumped phase conjugator, which uses a single crystal without external elements.[2] The true self-pumped phase conjugator is of potential interest because of its convenience for practical applications.[3] The first true self-pumped configuration was observed in 1982 by Feinberg in a single $BaTiO_3$ photorefractive crystal.[4] There are three different models to explain the origin of self-pumped phase conjugators in a signal photorefractive crystal (as shown in Fig. 1). In 1983, based on the experimental observation of the beam path in $BaTiO_3$ crystals, MacDonald and Feinberg[5] proposed a model that involved both four-wave mixing and total internal reflection (FWM-TIR) [see Fig. 1(a)]. In the model the phase conjugation is a result of FWM in two regions that are connected by TIR's from a corner of the crystal. Hence, a closed optical path loop is often observed inside the crystal. In 1985, Chang and Hellwarth[6] were the first to point out the close analogy between backward-stimulated Brillouin scattering and some configurations of self-pumped phase conjugation (SPPC) in $BaTiO_3$ and suggested that stimulated photorefractive backscattering (SPB) or stimulated two-wave mixing may be responsible for the generation of the SPPC [as shown in Fig. 1(b)]. It has been shown theoretically that the backward-scattered wave is dominated by the phase conjugate of the incident beam.[7,8] Recently we[9,10] proposed an alternative model of FWM-SPB (four-wave mixing and SPB, in which the SPB is produced by the formation of 2*k* gratings) to explain the SPPC observed in KTN:Fe and $BaTiO_3$:Ce crystals [as shown in Fig. 1(c)]. In this case the SPPC formation relies on both four FWM and SPB interactions. The phase-conjugate beam is generated by a four-wave-mixing process involving the incident beam, the forward-propagating beam (the fanning beam), and its backward-stimulated scattering beam. The backward-stimulated scattering beam is generated by the SPB process involving 2*k* gratings. Hence instead of a closed loop inside the crystal, filaments representing counter propagating beams are often observed.

In a typical SPPC experimental configuration, an extraordinarily polarized input beam is incident on the *a* face of a regular-cut $BaTiO_3$ photorefractive crystal. The SPPC formation mechanism is usually determined by the fanning pattern and the boundary conditions.[11] Generally speaking, SPPC is often generated by the SPB or the FWM-SPB mechanisms in some doped crystals but by the FWM-TIR mechanism in undoped crystals. This is mainly due to a significantly stronger fanning and larger coupling coefficients for 2*k* gratings in doped crystals. Changing the dopant concentration or the operat-

0740-3224/96/080000-08$10.00

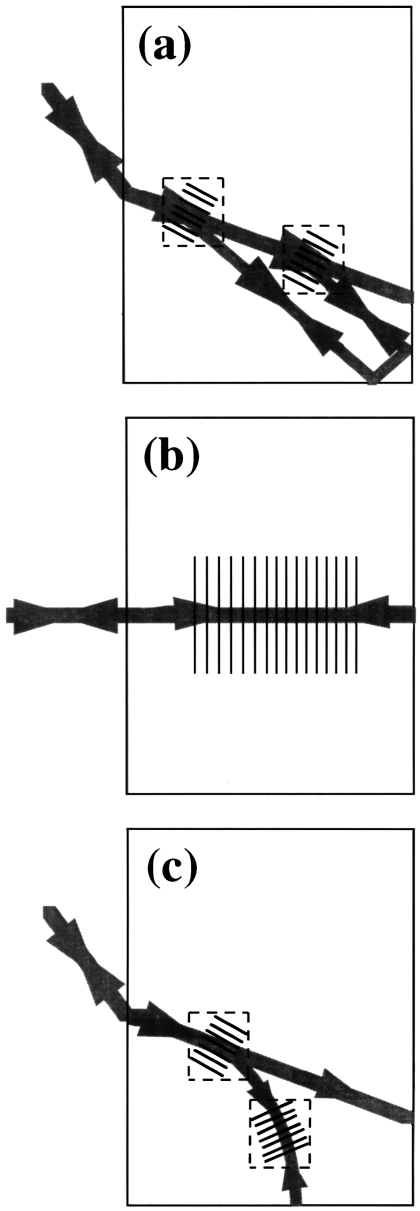

Fig. 1. Different modes of SPPC: (a) FWM-TIR, (b) SPB, and (c) FWM-SPB.

ing wavelength can cause a reconfiguration of the initial fanning pattern that leads to a change of the physical mechanism and the reflectivity of SPPC. Recently, we observed that the formation mechanism of SPPC was transformed from FWM-SPB to FWM-TIR when the wavelength of the input beam increased or the dopant concentration decreased.[12,13] We also observed that the mechanism transformation during SPPC and an enhancement of phase-conjugate reflectivity could be obtained by the variation of the polarization state of the input beam.[14] In a typical experiment an extraordinarily polarized input beam produces SPPC by FWM-SPB in a Ce:$BaTiO_3$ crystal. As the input polarization varies, the ordinary component, which serves as an erasing beam, decreases the effective coupling constant. This leads to a weaker fanning pattern. Depending on the boundary conditions, the fanned beam may reach the corner of the crystal cube, leading to SPPC by FWM-TIR. In this paper we theoretically and experimentally study the role of the $2k$ grating of SPB and the coupling strength of FWM in the FWM-SPB mode of self-pumped phase conjugators. A two-interaction-region approximation is used to theoretically calculate the reflectivity of phase conjugation and the threshold. We then present the results of our experimental studies, which validate the theoretical predictions. To vary the coupling constant, we also use an ordinarily incoherent erasing beam to reduce the index grating in the FWM and the SPB regions. The theoretical and the experimental results show that the reflectivity of phase conjugation depends strongly on the coupling strength of both the FWM and the SPB regions. In addition, the temporal dynamics of the phase-conjugate signal buildup process indicates that the $2k$ grating plays an important role in the FWM-SPB model. The paper can be organized as follows. In Section 2 we discuss a theoretical model of this new mode of SPPC. A closed-form solution of coupled-wave equations is obtained by use of an approximation. In Section 3 we discuss the experimental investigation using grating-erasure techniques at the two interaction regions to validate the theoretical predictions regarding the role of the $2k$ grating and the coupling strength of FWM during SPPC.

2. THEORETICAL ANALYSIS

Figure 2(a) shows a photograph of a typical optical beam path in the FWM-SPB mode of SPPC in Ce:$BaTiO_3$ crystals. Based on our experimental observation, the model of the FWM-SPB phase conjugator can be divided into two interactions regions, i.e., SPB and FWM interaction regions [as shown in Fig. 2(b)]. In the SPB interaction region there are two counterpropagating beams coupled by self-induced $2k$ gratings. The stimulated-backscattering beam A_2 is initially seeded by backscattering of fanned light from imperfection (pits) at the surface of the crystal. The backscattered light is amplified by SPB interaction with fanning beam A_1. These two beams provide the counterpropagating pump beams needed in the FWM for the generation of a phase-conjugate wave. Thus the SPB interaction region mainly acts as a feedback mirror (the SPB mirror, defined as the combination of the $2k$ grating gain region plus the scattering center) that provides one of the pump beams for the FWM interaction region. In the FWM interaction region, incident beam A_3, fanning beam A_1, and backscattering beam A_2 are coupled by a FWM interaction to generate a phase-conjugated beam A_4. For the phase-conjugation process to be sustained, the reflectivity of SPB region must be large enough to generate a self-oscillation between the SPB mirror and the FWM interaction region. Thus this phase conjugator is similar to a semilinear phase conjugator,[15] in which the mirror is replaced by a SPB mirror. The threshold and the reflectivity of a FWM-SPB phase conjugator are related to the net reflectivity of the SPB mirror.

We now treat this phase conjugator by using both optical FWM and contradirectional two-wave mixing in two separate regions. Referring to Fig. 2(b), we consider the interactions of all beams by using the following two sets of coupled equations. We consider only the transmission grating in the FWM region and the $2k$ grating in the SPB region. For the FWM interaction region the coupled

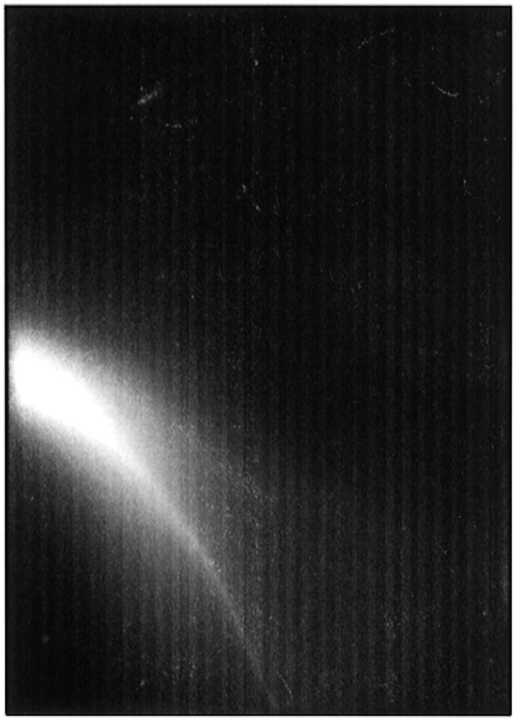

(a)

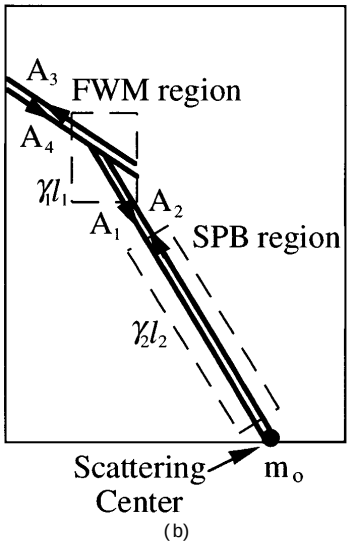

(b)

Fig. 2. FWM-SPB phase conjugator with a two-interaction region: (a) photograph of the optical beam path in a Ce:$BaTiO_3$ FWM-SPB phase conjugator; (b) theoretical model in which the forward-going fanning beam A_1 overlaps well with its backward-going scattering beam A_2 to form a SPB region. The amplified backscattering beam A_2 enters the FWM regions, mixes with A_1 and A_4, and generates the phase conjugate A_3.

equations are written as

$$\frac{dA_1}{dz} = \frac{\gamma_1}{2I_0}(A_1A_4^* + A_2^*A_3)A_4 - \frac{\gamma_2}{2I_0}A_1A_2^*A_2,$$

$$\frac{dA_2}{dz} = \frac{\gamma_1}{2I_0}(A_1^*A_4 + A_2A_3^*)A_3 - \frac{\gamma_2}{2I_0}A_1^*A_2A_1,$$

$$\frac{dA_3}{dz} = \frac{\gamma_1}{2I_0}(A_1A_4^* + A_2^*A_3)A_2,$$

$$\frac{dA_4}{dz} = \frac{\gamma_1}{2I_0}(A_1^*A_4 + A_2A_3^*)A_1, \qquad (1)$$

and for the SPB interaction region, the coupled equations are written as

$$\frac{dA_1}{dz'} = -\frac{\gamma_2}{2I_0'}A_1A_2^*A_2,$$

$$\frac{dA_2}{dz'} = -\frac{\gamma_2}{2I_0'}A_1^*A_2A_1, \qquad (2)$$

where γ_1 and γ_2 are the coupling constants of the transmission grating in the FWM region and the $2k$ grating in the SPB region, respectively. They are real and positive without the external electrical field in diffusion-dominant crystals, such as $BaTiO_3$, SBN, and KTN crystals. $I_0 = \sum_{j=1}^{4}|A_j|^2$ is the total intensity in the FWM region, and $I_0'(z') = \sum_{j=1}^{2}I_j(z') = \sum_{j=1}^{2}|A_j(z')|^2$ is the total intensity in the SPB region. The coordinate axis of the FWM region is defined as z, and that of the SPB region is defined as z'. These two regions are connected at $z' = 0$ or $z = l_1$, where l_1 is the interaction length of the FWM region and l_2 is the interaction length of the SPB region. In a typical FWM-SPB mode of self-pumped phase conjugation [as shown in Fig. 2(a)] the interaction length of the FWM region (l_1) is much smaller than that of the SPB region (l_2), but the γ_1 is much larger than γ_2 (in our case, $l_2 \approx 6l_1$ and $\gamma_1 \approx 5\gamma_2$). Hence these two sets of equations can be analytically solved by neglecting the $2k$ grating in the FWM region. In what follows, we first obtain the reflection generated by the SPB interaction by solving Eqs. (2). We then solve the coupled-mode equations in the FWM region by neglecting the $2k$-grating terms of Eq. (1). The phase-conjugate threshold and reflectivity of the FWM-SPB phase conjugator are obtained in terms of the coupling strength ($\gamma_2 l_2$) of SPB and that ($\gamma_1 l_1$) of FWM interaction.

A. Stimulated Photorefractive Backscattering Interaction Region

To examine the reflectivity of the SPB mirror, we first solve the coupled equations [Eqs. (2)] by following the procedure of contrapropagating two-wave mixing in Ref. 16 and by using the boundary condition $I_2(l_2)/I_1(l_2) = m_0$ at the surface of crystal (at $z' = l_2$), where m_0 is the backscattering coefficient of the imperfection on the surface of crystal. The solutions of Eqs. (2) are

$$I_1(z') = |A_1(z')|^2 = -C + \sqrt{C^2 + B\exp(-\gamma_2 z')},$$

$$I_2(z') = |A_2(z')|^2 = C + \sqrt{C^2 + B\exp(-\gamma_2 z')}, \qquad (3a)$$

where B and C are integration constants given by

$$B = I_1(l_2)I_2(l_2)\exp(-\gamma_2 l_2), \qquad C = \frac{I_2(l_2) - I_1(l_2)}{2}. \qquad (3b)$$

The effective intensity reflectivity of the SPB mirror, R, at $z' = 0$ (or $z = l_1$) can therefore be written

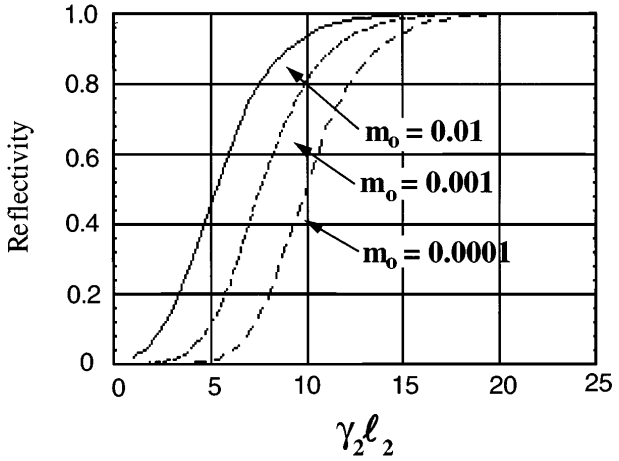

Fig. 3. Reflectivity of the SPB mirror as a function of $\gamma_2 l_2$ with various m_0.

$$R = \left|\frac{A_2(0)}{A_1(0)}\right|^2 = \frac{(1 - m_0)^2 + 2m_0 \exp(\gamma_2 l_2) - (1 - m_0)\sqrt{(1 - m_0)^2 + 4m_0 \exp(\gamma_2 l_2)}}{2m_0 \exp(\gamma_2 l_2)}. \quad (4)$$

When $m_0 \ll 1$, the reflectivity R can be written approximately as

$$R = \frac{1 + 2m_0 \exp(\gamma_2 l_2) - \sqrt{1 + 4m_0 \exp(\gamma_2 l_2)}}{2m_0 \exp(\gamma_2 l_2)}. \quad (5)$$

We note that R depends strongly on the product of m_0 and exponential factor $\exp(\gamma_2 l_2)$. According to Eq. (5), the presence of an efficient $2k$ grating ($\gamma_2 l_2 \gg 1$) is sufficient to achieve a high reflectivity even through the initial seeding m_0 from crystal-surface imperfection is very weak. The reflectivity of the SPB mirror reaches 100% when $\gamma_2 l_2$ approaches infinity. By use of Eq. (4), Fig. 3 plots the reflectivity of the SPB mirror as a function of $\gamma_2 l_2$ for various m_0. It can be seen that for a given small $\gamma_2 l_2$, the reflectivity R of the SPB mirror is very different for different m_0. When $\gamma_2 l_2$ increases, the difference is diminished and R reaches almost 100% when $\gamma_2 l_2 > 5$, while m_0 varies from 10^{-5} to 10^{-1}. This means that the amplification of a $2k$ grating provides an efficient mechanism to retroreflect the fanning beam into the FWM region to facilitate the phase-conjugation process.

B. Four-Wave-Mixing Interaction Region

With the reflectivity of the SPB mirror available we can now solve the coupled equations (1) in the FWM region by neglecting the $2k$ grating. Following a procedure similar to the one used in Ref. 1, we obtain the following expression for the phase-conjugate reflectivity:

$$\eta = \frac{|A_3(z = 0)|^2}{|A_4(z = 0)|^2} = \left(\frac{1 + \sigma}{1 - \sigma}\right)^2 \frac{1}{R}, \quad (6)$$

where R again is reflectivity of the SPB mirror, σ is the net power flow in this region, given by

$$\sigma = \frac{-1 \pm \sqrt{R^2 s^2 + Rs^2 - R}}{1 + R}, \quad (7)$$

and s can be obtained from the following transcendental equation, which is related to the coupling strength $\gamma_1 l_1$ of the FWM region:

$$\tanh \frac{\gamma_1 l_1}{4} s = s. \quad (8)$$

Equations (7) and (8) provide some constraints on $\gamma_1 l_1$ and s. We note that nontrivial solutions of the transcendental equation exist only when $\gamma_1 l_1 > 4$. Once s is solved, σ is determined by Eq. (7). Being a new power flow, σ has to be real. This requires $s^2 > 1/(1 + R)$. Thus if s or $\gamma_1 l_1$ are too small, there would be no phase conjugation. These constraints lead to a threshold coupling strength $(\gamma_1 l_1)_{\text{th}}$ and a threshold SPPC reflectivity η_{th} of the FWM-SPB phase conjugator, according to Eqs. (6) and (8), of

$$(\gamma_1 l_1)_{\text{th}} = 2\sqrt{1 + R} \ln\left(\frac{\sqrt{1 + R} + 1}{\sqrt{1 + R} - 1}\right), \quad (9)$$

$$\eta_{\text{th}} = \frac{R}{(1 + R)^2}. \quad (10)$$

We note that the phase-conjugate reflectivity is finite at threshold. Equation (9) shows that $(\gamma_1 l_1)_{\text{th}}$ is a decreasing function of R, reaching a minimum of 4.98 at $R = 1$. In order to further understand the concept, we plot $(\gamma_1 l_1)_{\text{th}}$ as a function of $\gamma_2 l_2$ for various scattering-center reflectivities m_0 (shown in Fig. 4). The SPPC reflectivity at threshold η_{th} is also plotted as a function of $\gamma_2 l_2$ for various m_0 (shown in Fig. 5). It can be seen that both m_0 and $\gamma_2 l_2$ influence greatly the threshold of the FWM-SPB phase conjugator. The threshold value of $(\gamma_1 l_1)_{\text{th}}$ decreases with m_0 and $\gamma_2 l_2$. The minimum value of 4.98 is almost the same as the threshold of the FWM-TIR phase conjugator (4.68 without loss, in which we should note that there is a factor of 2, according to our definition of the coupling constant).[17] It is also interesting to note that the reflectivity of SPPC at the threshold η_{th} is a decreasing function of $(\gamma_1 l_1)_{\text{th}}$. In general, the reflectivity of scattering center m_0 in the crystals is $\sim 10^{-3}$. An effective method to obtain a large SPB-mirror reflectivity R is to increase the coupling strength of the $2k$ grating $\gamma_2 l_2$

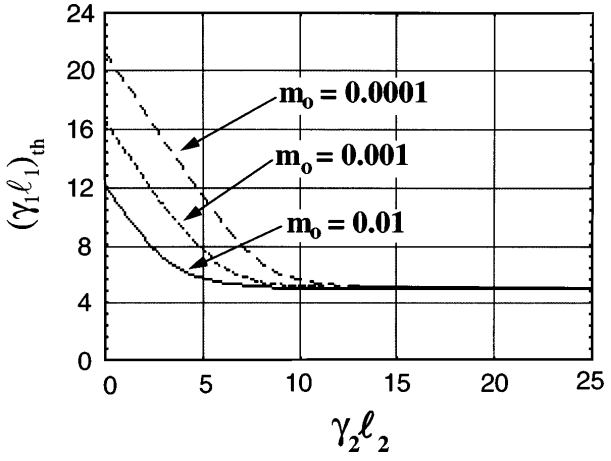

Fig. 4. Threshold coupling strength $(\gamma_1 l_1)_{\text{th}}$ of the FWM-SPB phase conjugator versus the coupling strength of the $2k$ grating $\gamma_2 l_2$ for various m_0.

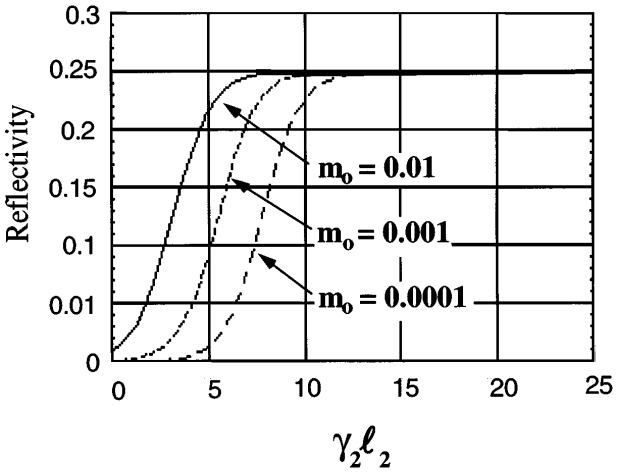

Fig. 5. SPPC reflectivity at threshold versus $\gamma_2 l_2$ for various m_0.

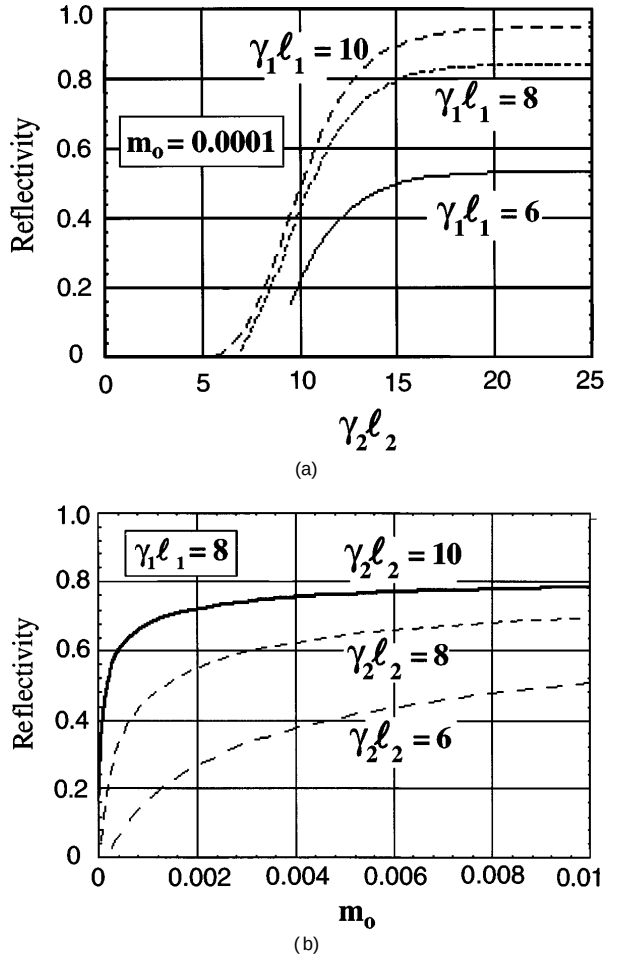

Fig. 6. Phase-conjugate reflectivity versus coupling strength of the $2k$ grating $\gamma_2 l_2$: (a) at different coupling strengths of the transmission grating $\gamma_1 l_1$ and (b) for various m_0.

(as shown in Fig. 3). This can be achieved by properly doping the crystals (e.g., Ce:$BaTiO_3$).

For $\gamma_1 l_1 > (\gamma_1 l_1)_{\text{th}}$ the reflectivity of the FWM-SPB phase conjugator η can be plotted as a function of $\gamma_2 l_2$ for the various $\gamma_1 l_1$ and m_0 [as shown in Figs. 6(a) and 6(b)]. We note that the reflectivity η obviously increases with $\gamma_2 l_2$ and behaves very differently for different $\gamma_1 l_1$. The reflectivity approaches a saturation value for a given $\gamma_1 l_1$, corresponding to a SPB-mirror reflectivity of $R = 100\%$ (at $\gamma_2 l_2 = \infty$). Referring to Fig. 3, we recall that SPB-mirror reflectivity R is an increasing function of $\gamma_2 l_2$, reaching $R = 100\%$ when $\gamma_2 l_2 = \infty$. We also note that all curves of different m_0 will approach the same saturation value when $\gamma_2 l_2 = \infty$. These figures confirm that the presence of a SPB $2k$ grating is essential to enhance the phase-conjugate reflectivity during SPPC. In order to increase the SPB-mirror reflectivity R, we can insert a retroreflecting screen into the path of the beam after the fanning beam leaves the crystal or use an artificial scattering center on the crystal face to increase m_0. We can also increase the coupling constant of $2k$ gratings by choosing an appropriate dopant and a proper wavelength. However, when the reflectivity of backscattering center m_0 is large enough, the phase-conjugate reflectivity is insensitive to the coupling strength of a $2k$ grating. For example, in the case of FWM-TIR, the corner cube is already providing a near 100% retroreflection regardless of the presence of $2k$ gratings. A small decrease of phase-conjugate reflectivity of ~20% was reported when the $2k$ grating was erased by an erasure beam in Ref. 18.

4. EXPERIMENT

In this section we report the results of our experiments to verify theoretical predictions based on the model of the FWM-SPB phase conjugator. The schematic diagram of the experimental arrangement is shown in Fig. 7. Our Ce-doped $BaTiO_3$ crystal has a red-orange color and a dopant concentration of approximately 30 parts in 10^6. The crystal is poled and 0° cut with dimensions 6.15 mm × 5.20 mm × 8.2 mm ($a \times b \times c$). An extraordinarily polarized beam from an argon laser (wavelength of 514.5 nm) is incident upon the crystal on the a face at an external angle of $\theta = 60°$. The phase conjugation was monitored by a calibrated photodiode (PD1). In order to investigate the buildup process of $2k$ gratings, the fanning beam was also monitored by another photodiode (PD2), and the optical path in the crystal was observed by imaging through the top of the crystal into a CCD camera. Figure 2(a) shows a photograph of the optical beam path inside the crystal during a typical mode of FWM-SPB SPPC. The input beam is depleted almost completely after propagating through a short distance and bends to the bottom surface of the crystal owing to the fanning effect. At steady state the end of the beam is characterized by a filament that is sustained through the SPB

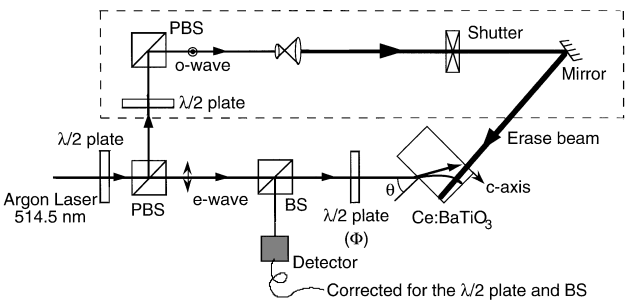

Fig. 7. Experimental setup used to demonstrate SPPC in the FWM-SPB mode: PBS's, polarizing beam splitters; BS's, beam splitters.

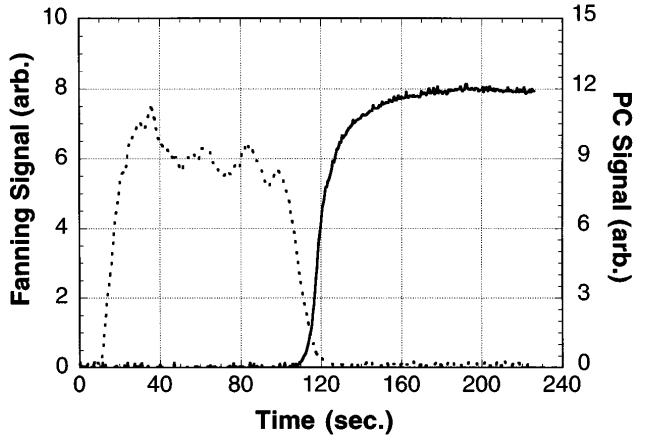

Fig. 8. Time evolution of the reflectivity of SPPC (solid curve) and intensity of the fanning beam (dashed curve).

process by $2k$ gratings. This SPPC formation is significantly different from the traditional FWM-TIR mechanism. There is no closed optical loop involving a corner inside the crystal.

Figure 8 shows the time evolution of the phase-conjugate signal (the solid curve) and the fanning signal (the dotted curve) during the buildup of the phase conjugation. At the first stage (t of 0–110 s, where $t = 0$ corresponds to the time when the incident beam is turned on), the fanning signal grows to a steady state, but the phase-conjugation signal only begins to start, as indicated by the recording at PD1. It indicates that at this moment, only the fanning beam is produced by the fanning grating in the FWM region, but the $2k$ grating has not been established in the SPB region. The forward fanning beam cannot be retroreflected into the FWM region to generate the phase conjugation. When $t > 110$ s, the phase-conjugation signal appears suddenly, while the fanning signal decreases significantly. This indicates the buildup of the $2k$ grating. After the fanning beam is produced by the incident beam, a backscattering can be generated by some defects on the surface of crystal, and the $2k$ grating can be written by the fanning beam and the retroreflected scattering beam. Once the $2k$ grating is formed, energy will be transformed from the fanning beam to the backscattering beam. With the increase of the backscattering, the amplitude of $2k$ grating also increases. This leads to more energy transfer from the fanning beam to the backscattering beam. The positive feedback provides the stimulated photorefractive backscattering and leads to some filaments at steady state. At the same time the backscattering beam will generate the phase conjugation by the FWM region and rewrite a new in-phase version of the fanning grating with the phase-conjugate beam to enhance the coupling in the FWM region. This explains the sharp rise of the phase conjugation as indicated in Fig. 8.

To further study the characteristics of the $2k$ grating in our model, we use an ordinarily polarized beam (see Fig. 7) that is incoherent with the input beam to illuminate the filaments uniformly in the SPB region. Since the refractive-index change of a photorefractive crystal is proportional to the modulation depth of the input light, the coupling coefficient of the $2k$ grating, $\gamma_2(I_r)$, can be written to incorporate the reduction in the modulation that results from the erasing beam,

$$\gamma_2(I_r) = \frac{\gamma_{2o}}{1 + I_r/I}, \tag{11}$$

where I is the total intensity in the filament, and γ_{2o} is the coupling-coefficient constant in the absence of the erasure beam I_r. According to the above equation, the coupling strength of the photorefractive grating can be easily controlled. Figure 9 shows the time evolution and the reflectivity of the phase-conjugate signal as the erasure beam is turned on. The signal decreases to different steady-state values depending on the intensity of erasure beams I_r. Figure 9 also shows that the reflectivity of the phase-conjugation signal decreases with the intensity of the erasing beam and exhibits a sharp threshold at $I_r = 4$ W/cm^2. To further illustrate the concept, we replot the phase-conjugate reflectivity as a function of $\gamma_2 l_2$, in which the intensity of the erasure beam can be calculated in terms of the coupling strength by use of Eq. (10). We also present the theoretical results by the dashed line in the figure for the purpose of comparison. The results are shown in Fig. 10, in which we estimate an average of I as 4 W/cm^2, a value of $\gamma_{2o} l_2$ as 11.5, a value of $\gamma_1 l_1$ as 7.0, and a reflectivity of scattering center m_0 as 0.001.

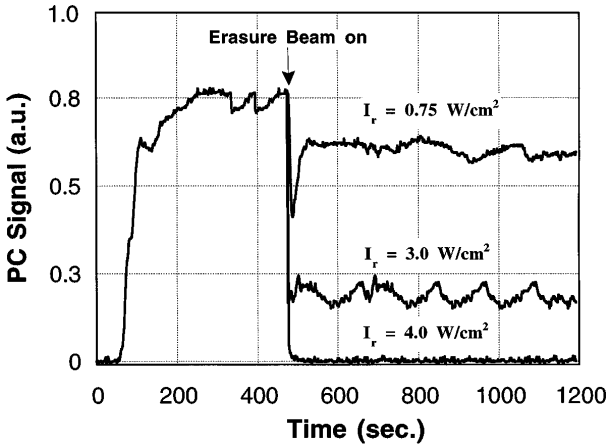

Fig. 9. Time-evolution of the phase-conjugate signal when the different erasing beams are applied.

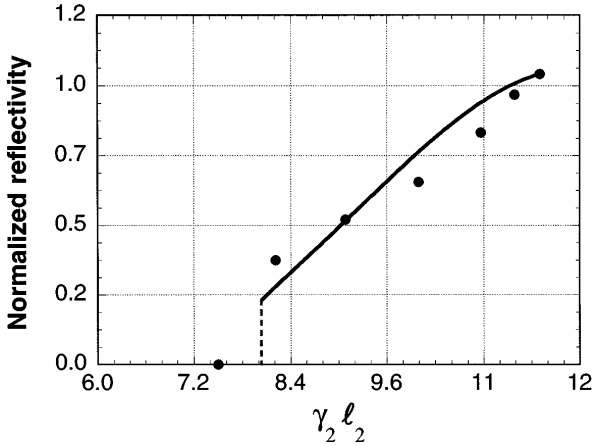

Fig. 10. Experimental phase-conjugate reflectivity versus $\gamma_2 l_2$. Note the phase-conjugate threshold at $\gamma_2 l_2 \approx 7.5$ (corresponding to $I_r = 4$ W/cm^2). The solid curve is from a theoretical calculation.

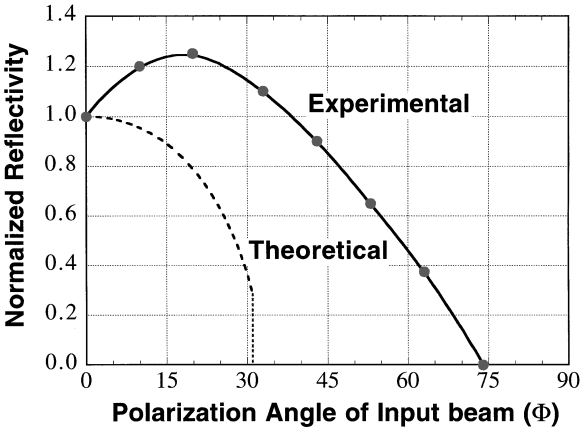

Fig. 11. Normalized phase-conjugation reflectivity as a function of the polarization angle, Φ, of the input beam. These experimental data are not corrected for Fresnel reflections. The dashed curve is from a theoretical calculation for a pure FWM-SPB mode of SPPC.

This curve is in agreement with the experimental results. Thus we note again that the presence of a $2k$-grating significantly affects the reflectivity of the backscattering beam and the SPPC in this model.

In a different experiment, to study the characteristic of the FWM region in this model, we block the erasing beam and introduce a general linear polarized input beam by inserting a half-wave plate in the path of the input beam (as shown in Fig. 7). The plane of polarization of the input beam could now be changed by rotating the half-wave plate. This leads to the presence of an ordinarily polarized component of the input beam. It is known that the coupling coefficient in Ce:$BaTiO_3$ crystal for an ordinarily polarized beam is much less than that of an extraordinarily polarized beam, and the cross coupling is negligible. Thus the extraordinarily polarized beam will contribute significantly to the fanning and the phase conjugation, whereas the ordinarily polarized beam will serve only to erase the gratings in the interaction regions. In this case the effective coupling coefficient of the grating, $\gamma_1(\phi)$, can be written as

$$\gamma_1(\phi) = \frac{\gamma_{1o}}{1 + \tan^2 \phi}, \tag{12}$$

where γ_{1o} is the coupling coefficient at $\phi = 0°$, where ϕ is the state of polarization of the input beam. It is defined (as shown in Fig. 7) as $\phi = 0°$ for the extraordinarily polarized direction and $\phi = 90°$ for the ordinarily polarized direction. The experimental (solid curve) and the theoretical (dashed curve) results of the reflectivity of phase conjugation are shown in Fig. 11. Here, we note that the phase-conjugate output is always extraordinarily polarized regardless of the input polarization state. The reflectivity of phase conjugation is therefore defined as the ratio of the conjugated signal and the extraordinary component of the incident beam. In other words, the reflectivity is normalized to that of a totally extraordinarily polarized state of the input beam ($\phi = 0°$). According to the theoretical prediction, the reflectivity will decrease with the ordinarily component of input beam. On the contrary, the experimental results show an improvement over the theoretical prediction. The reflectivity of phase conjugation exceeds the value at $\phi = 0°$ in the range $\phi < 35°$. The increase in phase-conjugate reflectivity can be caused by a mechanism transformation during SPPC.[14] In addition, the presence of an ordinarily polarized component in the input beam can restrain the self-generated fanning pattern. Thus the energy loss caused by fanning can be limited.

5. CONCLUSION

We have carried out a theoretical analysis of a FWM-SPB self-pumped phase conjugator by using two-interaction-region approximation. The phase-conjugate wave is generated by four-wave mixing with the assistance of $2k$ gratings by SPB. From our results, we find that the coupling strength $\gamma_2 l_2$ of the $2k$ grating in the SPB region and the feedback reflectivity m_0 of scattering centers play very important roles in the generation of the phase-conjugate wave. We have also presented the results of a comprehensive experimental investigation of a FWM-SPB phase conjugator by using two different types of erasing beam. We find that the phase conjugation of the FWM-SPB model relies on both the FWM and the SPB interactions.

ACKNOWLEDGMENT

This work is supported, in part, by the U.S. Office of Naval Research and the Air Force Office of Scientific Research. Pochi Yeh is also a principal technical advisor at Rockwell International Science Center, Thousand Oaks, California.

*Permanent address, Institute of Electro-Optical Engineering, National Chiao Tung University, Hsinchu, Taiwan.

†Current address, Lambda Research Optics, Inc., 17605 Fabrica, Suites A and B, Cerritos, California 90703.

REFERENCES

1. See, for example, P. Yeh, *Introduction to Photorefractive Nonlinear Optics* (Wiley, New York, 1993).
2. M. Cronin-Golomb, B. Fisher, J. O. White, and A. Yariv, "Theory and applications of four-wave mixing in photorefractive media," IEEE J. Quantum Electron. **QE-20,** 12 (1984).
3. See, for example, P. Gunter and J.-P. Huignard, eds., *Photorefractive Materials and Their Applications* (Springer-Verlag, Berlin, 1988), Vols. I and II.
4. J. Feinberg, "Self-pumped, continuous-wave phase conjugator using internal reflections," Opt. Lett. **42,** 919 (1983).
5. K. R. Macdonald and J. Feinberg, "Theory of a self-pumped phase conjugator with two coupled interaction regions," J. Opt. Soc. Am. **73,** 548 (1983).
6. T. Y. Chang and R. W. Hellwarth, "Optical phase conjugation by backscattering in barium titanate," Opt. Lett. **10,** 408 (1985).
7. J. F. Lam, "Origin of phase conjugate waves in self-pumped photorefractive mirrors," Appl. Phys. Lett. **46,** 909 (1985).
8. G. C. Valley, "Evolution of phase-conjugate waves in stimulated photorefractive backscattering," J. Opt. Soc. Am. B **9,** 1440 (1992).
9. Y. W. Lian, H. Gao, P. Ye, Q. Guan, and J. Wang, "Self-pumped phase conjugation with a new mechanism in $KTa_{1-x}Nb_xO_3$:Fe crystals," Appl. Phys. Lett. **63,** 1754 (1993).
10. Y. W. Lian, S. X. Dou, H. Gao, Y. Zhu, X. Wu, C. Yang, and P. Ye, "Mechanism transformation with wavelength of self-pumped phase conjugation in $BaTiO_3$:Ce," Opt. Lett. **19,** 610 (1994).

11. A. A. Zozulya, M. Saffman, and D. Z. Anderson, "Propagation of light beams in photorefractive media: fanning, self-bending, and formation of self-pumped four-wave-mixing phase conjugation geometries," Phys. Rev. Lett. **73,** 818 (1994).
12. Y. W. Lian, S. X. Dou, J. Zhang, H. Gao, Y. Zhu, X. Wu, C. Yang, and P. Ye, "Variation of mechanism transition wavelength of self-pumped phase conjugation with Ce-content in $BaTiO_3$:Ce crystals," Opt. Commun. **110,** 192 (1994).
13. Y. W. Lian, H. Gao, S. X. Dou, H. Wang, P. Ye, Q. Guan, and J. Wang, "Mechanism transition of self-pumped phase conjugation in $KTa_{1-x}Nb_xO_3$:Fe crystals," Appl. Phys. B **59,** 655 (1994).
14. Y. W. Lian, S. H. Lin, S. Campbell, K. Y. Hsu, P. Yeh, and Y. Zhu, "Polarization-dependent mechanism transformation during self-pumped phase conjugation in $BaTiO_3$:Ce," Opt. Lett. **20,** 1683 (1995).
15. M. Cronin-Golomb, B. Fisher, J. O. White, and A. Yariv, "Passing (self-pumped) phase conjugate mirror: theoretical and experimental investigation," Appl. Phys. Lett. **41,** 689 (1982).
16. P. Yeh, "Two-wave mixing in nonlinear media," IEEE J. Quantum Electron. **25,** 484 (1989).
17. Q. He, "Theory and applications of four-wave mixing in photorefractive media," IEEE J. Quantum Electron. **QE-24,** 2507 (1988).
18. G. L. Wood, E. J. Sharp, and G. J. Salamo, "Performance of photorefractive self-pumped phase conjugators," Proc. SPIE **1626,** 21 (1992).